

Bivariate density estimation using normal-gamma kernel with application
to astronomy

Uttam Bandyopadhyay¹ and Soumita Modak^{2,*}

Department of Statistics, University of Calcutta

35 Ballygunge Circular Road, Kolkata- 700019, India

email: ubandyopadhyay08@gmail.com¹, soumitamodak2013@gmail.com²

Abstract

We consider the problem of estimation of a bivariate density function with support $\mathfrak{R} \times [0, \infty)$, where a classical bivariate kernel estimator causes boundary bias due to the non-negative variable. To overcome this problem, we propose four kernel density estimators and compare their performances in terms of the mean integrated squared error. Simulation study shows that the estimator based on the proposed normal-gamma kernel performs best. Two astronomical data sets are used to demonstrate the applicability of this estimator.

keywords: Bivariate density estimation, Product of classical and gamma kernels, *NG* kernels, Astronomical application.

1 Introduction

Let $\mathbf{X}_i = (X_{i1}, \dots, X_{id})^T$, $i = 1, \dots, n$ be n independent realizations of d -dimensional random variable $\mathbf{X} = (X_1, \dots, X_d)^T$ having an unknown continuous d -variate probability density function f . In this chapter, we concentrate on the problem of estimating f by kernel density estimator, in which f with support \mathfrak{R}^d can be estimated by a d -variate classical kernel estimator (see, for example, Silverman, 1986; Wand and Jones, 1995). But this causes boundary bias in case of bounded or semi-bounded support. To solve this problem in univariate set-up, the associated kernels are proposed (see, for example, Chen, 1999, 2000; Libengué, 2013; Igarashi and Kakizawa, 2014), whereas, in multivariate set-up, the boundary bias can be omitted by using the product of d univariate associated kernels (see, for example, Bouerzmarni and Rombouts, 2010). In the context of multivariate associated kernel, Kokonendji and Somé (2018) propose a bivariate beta kernel with a correlation structure. Now, when the support is a cartesian product of \mathfrak{R} and bounded or semi-bounded sets, f can be estimated using the product of univariate classical

kernels and univariate associated kernels. Here, in particular, we consider the estimation of a bivariate density function with support $\mathfrak{R} \times [0, \infty)$.

In this regard, Section 2 contains the properties of the estimators based on the product of a univariate classical kernel and a univariate gamma kernel. Section 3 provides bivariate density estimators based on normal-gamma (*NG*) kernels. Section 4 discusses the relative performances of the estimators through simulation followed by data study in Section 5. Section 6 has the discussion, whereas some technical details are deferred to the Appendix.

2 Product of classical and gamma kernels

Consider a bivariate continuous density function f satisfying (i) $\mathbf{x} \in \mathfrak{R} \times [0, \infty)$, (ii) f is twice continuously partially differentiable on $\mathfrak{R} \times [0, \infty)$, (iii) $\int \{\partial f / \partial x_j\}^2 d\mathbf{x} < \infty, j = 1, 2$ and $\int \{x_2 \partial^2 f / \partial x_2^2\}^2 d\mathbf{x} < \infty$. To estimate f , we consider the estimator as follows

$$\hat{f}_1(\mathbf{x}) = \frac{1}{nh} \sum_{i=1}^n K\left(\frac{x_1 - X_{i1}}{h}\right) K_{x_2/b^2+1, b^2}(X_{i2}), \quad (1)$$

where K is the classical kernel satisfying (a) $K(-t) = K(t)$, (b) $\int_{-\infty}^{\infty} K(t) dt = 1$, (c) $\int_{-\infty}^{\infty} tK(t) dt = 0$ and (d) $\int_{-\infty}^{\infty} t^2 K(t) dt = k_2 \neq 0$, with bandwidth $h(> 0)$ satisfying $h \rightarrow 0$ and $nhb \rightarrow \infty$ as $n \rightarrow \infty$. $K_{x_2/b^2+1, b^2}$ is the first class of gamma kernels (Chen, 2000) defined as

$$K_{x_2/b^2+1, b^2}(t) = \frac{t^{x_2/b^2} e^{-t/b^2}}{b^{2(x_2/b^2+1)} \Gamma(x_2/b^2 + 1)},$$

where Γ is the gamma function, with bandwidth $b^2(> 0)$ satisfying $b \rightarrow 0$ and $nhb \rightarrow \infty$ as $n \rightarrow \infty$. Bandwidths of the kernels are so chosen as to make the amount of smoothing in the same scale for both the kernels. In general, any associated kernel can be used here. However, we choose the gamma kernel due to its flexible properties (see, for example, Chen, 2000).

Now, using $y_1 = x_1 - ht$, we get

$$\begin{aligned}
E\{\hat{f}_1(\mathbf{x})\} &= \int_{-\infty}^{\infty} \int_0^{\infty} \left[h^{-1} K\left(\frac{x_1 - y_1}{h}\right) \right] K_{x_2/b^2+1, b^2}(y_2) f(y_1, y_2) dy_1 dy_2 \\
&= \int_{-\infty}^{\infty} \int_0^{\infty} K(t) K_{x_2/b^2+1, b^2}(y_2) f(x_1 - ht, y_2) dt dy_2 \\
&= \int_{-\infty}^{\infty} K(t) E_{\xi_{x_2}}[f(x_1 - ht, y_2)] dt, \tag{2}
\end{aligned}$$

where ξ_{x_2} follows $\text{gamma}(x_2/b^2 + 1, b^2)$.

Again, Taylor series expansion gives $E_{\xi_{x_2}}[f(x_1 - ht, \xi_{x_2})]$ as

$$\begin{aligned}
&f(x_1, x_2) + E_{\xi_{x_2}}(x_1 - ht - x_1) f^1(\mathbf{x}) + E_{\xi_{x_2}}(\xi_{x_2} - x_2) f^2(\mathbf{x}) \\
&+ \frac{1}{2} E_{\xi_{x_2}}\{(x_1 - ht - x_1)^2\} f^{11}(\mathbf{x}) + \frac{1}{2} E_{\xi_{x_2}}\{(\xi_{x_2} - x_2)^2\} f^{22}(\mathbf{x}) \\
&+ \frac{1}{2} E_{\xi_{x_2}}\{(-ht)(\xi_{x_2} - x_2)\} f^{12}(\mathbf{x}) + \frac{1}{2} E_{\xi_{x_2}}\{(-ht)(\xi_{x_2} - x_2)\} f^{21}(\mathbf{x}) \\
&+ o(h^2 + b^2) \\
&= f(\mathbf{x}) - ht f^1(\mathbf{x}) + E_{\xi_{x_2}}(\xi_{x_2} - x_2 - b^2) f^2(\mathbf{x}) + b^2 f^2(\mathbf{x}) \\
&+ \frac{1}{2} h^2 t^2 f^{11}(\mathbf{x}) + \frac{1}{2} \text{Var}(\xi_{x_2}) f^{22}(\mathbf{x}) + o(h^2 + b^2),
\end{aligned}$$

where $f^j = \partial f / \partial x_j$ and $f^{jj'} = \partial^2 f / \partial x_j \partial x_{j'}$, $j, j' = 1, 2$. Then, substituting the last expression in (2), we get

$$E\{\hat{f}_1(\mathbf{x})\} = f(\mathbf{x}) + \frac{1}{2} k_2 h^2 f^{11}(\mathbf{x}) + b^2 \{f^2(\mathbf{x}) + \frac{1}{2} x_2 f^{22}(\mathbf{x})\} + o(h^2 + b^2),$$

which implies $\text{Bias}\{\hat{f}_1(\mathbf{x})\}$ is

$$\frac{1}{2} k_2 h^2 f^{11}(\mathbf{x}) + b^2 \{f^2(\mathbf{x}) + \frac{1}{2} x_2 f^{22}(\mathbf{x})\} + o(h^2 + b^2) = O(h^2 + b^2). \tag{3}$$

This shows estimator \hat{f}_1 is free of boundary bias and the corresponding integrated squared bias is given by

$$\begin{aligned}
&\int \{\text{Bias}(\hat{f}_1(\mathbf{x}))\}^2 d\mathbf{x} \\
&= \frac{1}{4} k_2^2 h^4 \int \{f^{11}(\mathbf{x})\}^2 d\mathbf{x} + b^4 \int \{f^2(\mathbf{x}) + \frac{1}{2} x_2 f^{22}(\mathbf{x})\}^2 d\mathbf{x} \\
&+ k_2 h^2 b^2 \int f^{11}(\mathbf{x}) \{f^2(\mathbf{x}) + \frac{1}{2} x_2 f^{22}(\mathbf{x})\} d\mathbf{x} + o(h^4 + b^4). \tag{4}
\end{aligned}$$

Now,

$$\begin{aligned}
Var\{\hat{f}_1(\mathbf{x})\} &= n^{-1}Var\{K(X_{i1})K_{x_2/b^2+1,b^2}(X_{i2})\} \\
&= n^{-1}E\{K(X_{i1})K_{x_2/b^2+1,b^2}(X_{i2})\}^2 + O(n^{-1}) \\
&= n^{-1}h^{-1}\int_{-\infty}^{\infty}\int_0^{\infty}K^2(t)K_{x_2/b^2+1,b^2}^2(y_2)f(x_1 - ht, y_2)dtdy_2 \\
&\quad + O(n^{-1})
\end{aligned}$$

and

$$\int_0^{\infty}K_{x_2/b^2+1,b^2}^2(y_2)f(x_1 - ht, y_2)dy_2 = B_b(x_2)E_{\eta_{x_2}}\{f(x_1 - ht, \eta_{x_2})\},$$

where η_{x_2} follows gamma($2x_2/b^2 + 1, b^2$) and $B_b(x_2) = \frac{b^{-2}\Gamma(2x_2/b^2+1)}{2^{2x_2/b^2+1}\Gamma^2(x_2/b^2+1)}$. Lemma 3 of Brown and Chen (1999) gives

$$B_b(x_2) \sim \begin{cases} \frac{1}{2\sqrt{\pi}}b^{-1}x^{-1/2} & \text{if } \frac{x_2}{b^2} \rightarrow \infty, \\ \frac{\Gamma(2\kappa + 1)}{2^{1+2\kappa}\Gamma^2(\kappa + 1)}b^{-2} & \text{if } \frac{x_2}{b^2} \rightarrow \kappa \text{ (a non-negative constant),} \end{cases}$$

which implies

$$Var\{\hat{f}_1(\mathbf{x})\} \sim \begin{cases} \frac{1}{2\sqrt{\pi}}n^{-1}h^{-1}b^{-1}k_3x_2^{-1/2}f(\mathbf{x}) & \text{if } \frac{x_2}{b^2} \rightarrow \infty, \\ \frac{\Gamma(2\kappa + 1)}{2^{1+2\kappa}\Gamma^2(\kappa + 1)}n^{-1}h^{-1}b^{-2}k_3f(\mathbf{x}) & \text{if } \frac{x_2}{b^2} \rightarrow \kappa, \end{cases} \quad (5)$$

where $k_3 = \int_{-\infty}^{\infty}K^2(t)dt$. Expressions (3) and (5) imply that for $h \rightarrow 0, b \rightarrow 0$, and $nhb \rightarrow \infty$ as $n \rightarrow \infty$, the nonparametric density estimator $\hat{f}_1(\mathbf{x})$ is consistent for the true density function $f(\mathbf{x})$ at each point \mathbf{x} . Now, for

$\delta = b^{2-\epsilon}$ with $1 < \epsilon < 2$,

$$\begin{aligned}
& \int_{-\infty}^{\infty} \int_0^{\infty} \text{Var}\{\hat{f}_1(\mathbf{x})\} dx_1 dx_2 \\
&= \int_{-\infty}^{\infty} \int_0^{\delta} \text{Var}\{\hat{f}_1(\mathbf{x})\} dx_1 dx_2 + \int_{-\infty}^{\infty} \int_{\delta}^{\infty} \text{Var}\{\hat{f}_1(\mathbf{x})\} dx_1 dx_2 \\
&= \frac{1}{2\sqrt{\pi}} n^{-1} h^{-1} b^{-1} k_3 \int_{-\infty}^{\infty} \int_{\delta}^{\infty} x_2^{-1/2} f(\mathbf{x}) dx_1 dx_2 + O(n^{-1} h^{-1} b^{-\epsilon}) \\
&= \frac{1}{2\sqrt{\pi}} n^{-1} h^{-1} b^{-1} k_3 \int_{-\infty}^{\infty} \int_0^{\infty} x_2^{-1/2} f(\mathbf{x}) dx_1 dx_2 + o(n^{-1} h^{-1} b^{-1}), \quad (6)
\end{aligned}$$

provided $\int_{-\infty}^{\infty} \int_0^{\infty} x_2^{-1/2} f(\mathbf{x}) dx_1 dx_2$ is finite.

Combining (4) and (6), the mean integrated squared error (MISE) is obtained as

$$\begin{aligned}
\text{MISE}\{\hat{f}_1(\mathbf{x})\} &= \int \{\text{Bias}(f_1(\mathbf{x}))\}^2 d\mathbf{x} + \int \text{Var}\{\hat{f}_1(\mathbf{x})\} d\mathbf{x} \\
&= \frac{1}{4} k_2^2 h^4 \int \{f^{11}(\mathbf{x})\}^2 d\mathbf{x} + b^4 \int \{f^2(\mathbf{x}) + \frac{1}{2} x_2 f^{22}(\mathbf{x})\}^2 d\mathbf{x} \\
&\quad + k_2 h^2 b^2 \int f^{11}(\mathbf{x}) \{f^2(\mathbf{x}) + \frac{1}{2} x_2 f^{22}(\mathbf{x})\} d\mathbf{x} \\
&\quad + \frac{1}{2\sqrt{\pi}} n^{-1} h^{-1} b^{-1} k_3 \int x_2^{-1/2} f(\mathbf{x}) d\mathbf{x} + o(n^{-1} h^{-1} b^{-1} + h^4 + b^4) \quad (7)
\end{aligned}$$

and the leading terms in (7) give the expression of the corresponding asymptotic mean integrated squared error (AMISE). AMISE is optimal for $h_{opt} = h_0 n^{-1/6}$ and $b_{opt} = b_0 n^{-1/6}$, where h_0 and b_0 are constants, i.e. the optimal bandwidths for kernel density estimator \hat{f}_1 are $O(n^{-1/6})$ and $O(n^{-1/3})$ which give $\text{AMISE}\{\hat{f}_1(\mathbf{x})\}_{opt}$ as

$$\begin{aligned}
& \left[\frac{1}{4} k_2^2 h_0^4 \int \{f^{11}(\mathbf{x})\}^2 d\mathbf{x} + b_0^4 \int \{f^2(\mathbf{x}) + \frac{1}{2} x_2 f^{22}(\mathbf{x})\}^2 d\mathbf{x} \right. \\
&\quad + k_2 h_0^2 b_0^2 \int f^{11}(\mathbf{x}) \{f^2(\mathbf{x}) + \frac{1}{2} x_2 f^{22}(\mathbf{x})\} d\mathbf{x} \\
&\quad \left. + \frac{1}{2\sqrt{\pi}} n^{-1} h_0^{-1} b_0^{-1} k_3 \int x_2^{-1/2} f(\mathbf{x}) d\mathbf{x} \right] n^{-2/3}.
\end{aligned}$$

For $h = b = h_0$, the optimal h_0 is

$$\left[\frac{\frac{1}{2\sqrt{\pi}}k_3 \int x_2^{-1/2} f(\mathbf{x}) d\mathbf{x}}{2 \int \left\{ \frac{1}{2}k_2 f^{11}(\mathbf{x}) + f^2(\mathbf{x}) + \frac{1}{2}x_2 f^{22}(\mathbf{x}) \right\}^2 d\mathbf{x}} \right]^{1/6} n^{-1/6},$$

which gives $AMISE_{opt}$ as

$$\frac{3}{2^{2/3}} \left[\int \left\{ \frac{1}{2}k_2 f^{11}(\mathbf{x}) + f^2(\mathbf{x}) + \frac{1}{2}x_2 f^{22}(\mathbf{x}) \right\}^2 d\mathbf{x} \right]^{1/3} \left[\frac{1}{2\sqrt{\pi}}k_3 \int x_2^{-1/2} f(\mathbf{x}) d\mathbf{x} \right]^{2/3} n^{-2/3}.$$

Another estimator of f is considered as

$$\hat{f}_2(\mathbf{x}) = \frac{1}{nh} \sum_{i=1}^n K\left(\frac{x_1 - X_{i1}}{h}\right) K_{\rho_{b^2}(x_2), b^2}(X_{i2}), \quad (8)$$

where $K_{\rho_{b^2}(x), b^2}$ is the second class of gamma kernels (Chen, 2000) defined as

$$\rho_{b^2}(x_2) = \begin{cases} x_2/b^2 & \text{if } x_2 \geq 2b^2, \\ \frac{1}{4}(x_2/b^2)^2 + 1 & \text{if } x_2 \in [0, 2b^2]. \end{cases} \quad (9)$$

So, $Bias\{\hat{f}_2(\mathbf{x})\}$, given by

$$\begin{cases} \frac{1}{2}k_2 h^2 f^{11}(\mathbf{x}) + \frac{1}{2}b^2 x_2 f^{22}(\mathbf{x}) + o(h^2 + b^2) & \text{if } x_2 \geq 2b^2, \\ \frac{1}{2}k_2 h^2 f^{11}(\mathbf{x}) + b^2 \{\rho_{b^2}(x_2) - x_2/b^2\} f^2(\mathbf{x}) & \text{if } x_2 \in [0, 2b^2), \\ +o(h^2 + b^2) & \end{cases} \quad (10)$$

which shows the boundary unbiasedness of estimator \hat{f}_2 and for a non-negative constant κ ,

$$Var\{\hat{f}_2(\mathbf{x})\} \sim \begin{cases} \frac{1}{2\sqrt{\pi}} n^{-1} h^{-1} b^{-1} k_3 x_2^{-1/2} f(\mathbf{x}) & \text{if } \frac{x_2}{b^2} \rightarrow \infty, \\ \frac{\Gamma(\kappa^2/2 + 1)}{2^{1+\kappa^2/2} \Gamma^2(\kappa^2/4 + 1)} n^{-1} h^{-1} b^{-2} k_3 f(\mathbf{x}) & \text{if } \frac{x_2}{b^2} \rightarrow \kappa, \end{cases}$$

imply

$$\begin{aligned} MISE\{\hat{f}_2(\mathbf{x})\} &= \frac{1}{4}k_2^2h^4 \int \{f^{11}(\mathbf{x})\}^2 d\mathbf{x} + \frac{1}{4}b^4 \int \{x_2f^{22}(\mathbf{x})\}^2 d\mathbf{x} \\ &+ \frac{1}{2}k_2h^2b^2 \int f^{11}(\mathbf{x})\{x_2f^{22}(\mathbf{x})\}d\mathbf{x} + o(h^4 + b^4) \\ &+ \frac{1}{2\sqrt{\pi}}n^{-1}h^{-1}b^{-1}k_3 \int x_2^{-1/2}f(\mathbf{x})d\mathbf{x} + o(n^{-1}h^{-1}b^{-1}). \end{aligned}$$

For $h = b = h_0$, the optimal h_0 is

$$\left[\frac{\frac{1}{2\sqrt{\pi}}k_3 \int x_2^{-1/2}f(\mathbf{x})d\mathbf{x}}{\frac{1}{2} \int \{k_2f^{11}(\mathbf{x}) + x_2f^{22}(\mathbf{x})\}^2 d\mathbf{x}} \right]^{1/6} n^{-1/6},$$

which corresponds to $AMISE_{opt}$, given by

$$\frac{3}{2^{4/3}} \left[\int \left\{ k_2f^{11}(\mathbf{x}) + x_2f^{22}(\mathbf{x}) \right\}^2 d\mathbf{x} \right]^{1/3} \left[\frac{1}{2\sqrt{\pi}}k_3 \int x_2^{-1/2}f(\mathbf{x})d\mathbf{x} \right]^{2/3} n^{-2/3}.$$

Observe that $AMISE_{opt}\{\hat{f}_1(\mathbf{x})\} \geq AMISE_{opt}\{\hat{f}_2(\mathbf{x})\}$ implies \hat{f}_2 is expected to have a better asymptotic performance than \hat{f}_1 .

3 Bivariate density estimation using NG kernel

Consider the density function K_{Θ} of a bivariate normal-gamma distribution defined as (Bernardo and Smith, 2000)

$$\begin{aligned} K_{\Theta}(t_1, t_2) &= NG(t_1, t_2|\Theta = (\mu, \lambda, \alpha, \beta)) = N(t_1|\mu, (\lambda t_2)^{-1})Ga(t_2|\alpha, \beta) \\ &= \sqrt{\frac{\lambda t_2}{2\pi}} e^{-\frac{(t_1-\mu)^2 \lambda t_2}{2}} \times \frac{\beta^\alpha}{\Gamma(\alpha)} t_2^{\alpha-1} e^{-\beta t_2} \end{aligned} \quad (11)$$

with $\mu \in \Re, \lambda > 0, \alpha > 0, \beta > 0$, where N and Ga , respectively, stand for normal and gamma distributions. Using (11), we define the following estimator of f as

$$\hat{f}_3(\mathbf{x}) = \frac{1}{n} \sum_{i=1}^n K_{\Theta_1}(\mathbf{X}_i), \quad (12)$$

where K_{Θ_1} is the NG kernel with $\Theta = \Theta_1 = (x_1, 1/(|x_1|b_1 + b_1^2)(x_2 + b_2), x_2/b_2 + 2, 1/b_2)$ such that the bandwidths $b_1, b_2 \rightarrow 0$ and $nb_1b_2 \rightarrow \infty$ as $n \rightarrow \infty$. Then,

$$E\{\hat{f}_3(\mathbf{x})\} = \int K_{\Theta_1}(\mathbf{y})d\mathbf{y} = E\{f(\boldsymbol{\xi}_x)\},$$

where $\boldsymbol{\xi}_x = (\xi_{x_1}, \xi_{x_2})^T$ follows $NG(\xi_{x_1}, \xi_{x_2}|x_1, 1/(|x_1|b_1 + b_1^2)(x_2 + b_2), x_2/b_2 + 2, 1/b_2)$, which implies $E(\xi_{x_1}) = x_1, E(\xi_{x_2}) = x_2 + 2b_2, Var(\xi_{x_1}) = |x_1|b_1 + b_1^2$ and $Var(\xi_{x_2}) = x_2b_2 + 2b_2^2$. By Taylor series expansion we get (see, Appendix A.1),

$$\begin{aligned} E\{f(\boldsymbol{\xi}_x)\} &= f(\mathbf{x}) + E(\xi_{x_1} - x_1)f^1(\mathbf{x}) + E(\xi_{x_2} - x_2)f^2(\mathbf{x}) \\ &\quad + \frac{1}{2}E\{(\xi_{x_1} - x_1)(\xi_{x_2} - x_2)\}\{f^{12}(\mathbf{x}) + f^{21}(\mathbf{x})\} \\ &\quad + \frac{1}{2}E(\xi_{x_1} - x_1)^2f^{11}(\mathbf{x}) + \frac{1}{2}E(\xi_{x_2} - x_2)^2f^{22}(\mathbf{x}) + o(b_1 + b_2) \\ &= f(\mathbf{x}) + b_1\left\{\frac{1}{2}|x_1|f^{11}(\mathbf{x})\right\} + b_2\left\{2f^2(\mathbf{x}) + \frac{1}{2}x_2f^{22}(\mathbf{x})\right\} + o(b_1 + b_2). \end{aligned}$$

Therefore, $Bias\{\hat{f}_3(\mathbf{x})\}$ is given by

$$b_1\left\{\frac{1}{2}|x_1|f^{11}(\mathbf{x})\right\} + b_2\left\{2f^2(\mathbf{x}) + \frac{1}{2}x_2f^{22}(\mathbf{x})\right\} + o(b_1 + b_2) = O(b_1 + b_2), \quad (13)$$

which shows estimator \hat{f}_3 is free of boundary bias, and the integrated squared bias is

$$\begin{aligned} &\int \{Bias(\hat{f}_3(\mathbf{x}))\}^2 d\mathbf{x} \\ &= \frac{1}{4}b_1^2 \int \{x_1f^{11}(\mathbf{x})\}^2 d\mathbf{x} + b_2^2 \int \{2f^2(\mathbf{x}) + \frac{1}{2}x_2f^{22}(\mathbf{x})\}^2 d\mathbf{x} \\ &\quad + b_1b_2 \int \{|x_1|f^{11}(\mathbf{x})\}\{2f^2(\mathbf{x}) + \frac{1}{2}x_2f^{22}(\mathbf{x})\} d\mathbf{x} + o(b_1^2 + b_2^2). \quad (14) \end{aligned}$$

The variance of $\hat{f}_3(\mathbf{x})$ is

$$Var\{\hat{f}_3(\mathbf{x})\} \sim \begin{cases} \frac{1}{4\pi\sqrt{e}}n^{-1}b_1^{-1/2}b_2^{-1/2}|x_1|^{-1/2}x_2^{-1/2}f(\mathbf{x}) & \text{if } |x_1|/b_1 \rightarrow \infty, x_2/b_2 \rightarrow \infty, \\ \frac{\Gamma(2\kappa_2 + 7/2)}{\sqrt{\pi}2^{2\kappa_2+9/2}\sqrt{(\kappa_1+1)(\kappa_2+1)}\Gamma^2(\kappa_2+2)}n^{-1}b_1^{-1}b_2^{-1}f(\mathbf{x}) & \text{if } |x_1|/b_1 \rightarrow \kappa_1, x_2/b_2 \rightarrow \kappa_2, \\ \frac{\Gamma(2\kappa_2 + 7/2)}{\sqrt{\pi}2^{2\kappa_2+9/2}\sqrt{(\kappa_2+1)}\Gamma^2(\kappa_2+2)}n^{-1}b_1^{-1/2}b_2^{-1}|x_1|^{-1/2}f(\mathbf{x}) & \text{if } |x_1|/b_1 \rightarrow \infty, x_2/b_2 \rightarrow \kappa_2, \\ \frac{1}{4\pi\sqrt{e}\sqrt{\kappa_1+1}}n^{-1}b_1^{-1}b_2^{-1/2}x_2^{-1/2}f(\mathbf{x}) & \text{if } |x_1|/b_1 \rightarrow \kappa_1, x_2/b_2 \rightarrow \infty, \end{cases}$$

for non-negative constants κ_1, κ_2 (see, Appendix A.2), and

$$\begin{aligned} & \int \text{Var}\{\hat{f}_3(\mathbf{x})\} d\mathbf{x} \\ &= \frac{1}{4\pi\sqrt{e}} n^{-1} b_1^{-1/2} b_2^{-1/2} \int |x_1|^{-1/2} x_2^{-1/2} f(\mathbf{x}) d\mathbf{x} + o(n^{-1} b_1^{-1/2} b_2^{-1/2}), \end{aligned} \quad (15)$$

assuming $\int |x_1|^{-1/2} x_2^{-1/2} f(\mathbf{x}) d\mathbf{x} < \infty$ (see, Appendix A.3).

Now, combining (14) and (15), we get the expression of the MISE as follows

$$\begin{aligned} \text{MISE}\{\hat{f}_3(\mathbf{x})\} &= \frac{1}{4} b_1^2 \int \{|x_1| f^{11}(\mathbf{x})\}^2 d\mathbf{x} + b_2^2 \int \{2f^2(\mathbf{x}) + \frac{1}{2} x_2 f^{22}(\mathbf{x})\}^2 d\mathbf{x} \\ &\quad + b_1 b_2 \int |x_1| f^{11}(\mathbf{x}) \{2f^2(\mathbf{x}) + \frac{1}{2} x_2 f^{22}(\mathbf{x})\} d\mathbf{x} \\ &\quad + \frac{1}{4\pi\sqrt{e}} n^{-1} b_1^{-1/2} b_2^{-1/2} \int |x_1|^{-1/2} x_2^{-1/2} f(\mathbf{x}) d\mathbf{x} \\ &\quad + o(b_1^2 + b_2^2 + n^{-1} b_1^{-1/2} b_2^{-1/2}). \end{aligned}$$

For $b_1 = b_2 = b_0$, the optimal b_0 is given by

$$\left[\frac{\frac{1}{4\pi\sqrt{e}} \int |x_1|^{-1/2} x_2^{-1/2} f(\mathbf{x}) d\mathbf{x}}{2 \int \left\{ \frac{1}{2} |x_1| f^{11}(\mathbf{x}) + 2f^2(\mathbf{x}) + \frac{1}{2} x_2 f^{22}(\mathbf{x}) \right\}^2 d\mathbf{x}} \right]^{1/3} n^{-1/3},$$

for which the optimal AMISE is obtained as

$$\begin{aligned} \text{AMISE}_{opt} &= \frac{3}{2^{2/3}} \left[\int \left\{ \frac{1}{2} |x_1| f^{11}(\mathbf{x}) + 2f^2(\mathbf{x}) + \frac{1}{2} x_2 f^{22}(\mathbf{x}) \right\}^2 d\mathbf{x} \right]^{1/3} \\ &\quad \left[\frac{1}{4\pi\sqrt{e}} \int |x_1|^{-1/2} x_2^{-1/2} f(\mathbf{x}) d\mathbf{x} \right]^{2/3} n^{-2/3}. \end{aligned}$$

We propose another estimator of f using (11) as follows

$$\hat{f}_4(\mathbf{x}) = \frac{1}{n} \sum_{i=1}^n K_{\Theta_2}(\mathbf{X}_i), \quad (16)$$

where K_{Θ_2} is the NG kernel with $\Theta = \Theta_2 = (x_1, 1/(|x_1|b_1 + b_1^2))(x_2 + b_2), \alpha_{b_2}(x_2), 1/b_2)$ and

$$\alpha_{b_2}(x_2) = \begin{cases} x_2/b_2 & \text{if } x_2 \geq 3b_2, \\ \frac{1}{9}(x_2/b_2)^2 + 2 & \text{if } x_2 \in [0, 3b_2), \end{cases}$$

such that $b_1, b_2 \rightarrow 0, nb_1b_2 \rightarrow \infty$ as $n \rightarrow \infty$. Then, in the similar fashion as in estimator \hat{f}_3 , we obtain $Bias\{\hat{f}_4(\mathbf{x})\}$ as

$$\begin{cases} \frac{1}{2}\{b_1|x_1|f^{11}(\mathbf{x}) + b_2x_2f^{22}(\mathbf{x})\} + o(b_1 + b_2) & \text{if } x_2 \geq 3b_2, \\ \frac{1}{2}b_1|x_1|f^{11}(\mathbf{x}) + b_2\{\alpha_{b_2}(x_2) - \frac{x_2}{b_2}\}f^2(\mathbf{x}) + o(b_1 + b_2) & \text{if } x_2 \in [0, 3b_2), \end{cases}$$

establishing its boundary unbiasedness, and

$$Var\{\hat{f}_4(\mathbf{x})\} \sim \begin{cases} \frac{1}{4\pi\sqrt{e}}n^{-1}b_1^{-1/2}b_2^{-1/2}|x_1|^{-1/2}x_2^{-1/2}f(\mathbf{x}) & \text{if } |x_1|/b_1 \rightarrow \infty, \quad x_2/b_2 \rightarrow \infty, \\ \frac{\Gamma(2/9\kappa_2^2+7/2)}{\sqrt{\pi}2^{2/9\kappa_2^2+9/2}\sqrt{(\kappa_1+1)(\kappa_2+1)}\Gamma^2(1/9\kappa_2^2+2)}n^{-1}b_1^{-1}b_2^{-1}f(\mathbf{x}) & \text{if } |x_1|/b_1 \rightarrow \kappa_1, \quad x_2/b_2 \rightarrow \kappa_2, \\ \frac{\Gamma(2/9\kappa_2^2+7/2)}{\sqrt{\pi}2^{2/9\kappa_2^2+9/2}\sqrt{(\kappa_2+1)}\Gamma^2(1/9\kappa_2^2+2)}n^{-1}b_1^{-1/2}b_2^{-1}|x_1|^{-1/2}f(\mathbf{x}) & \text{if } |x_1|/b_1 \rightarrow \infty, \quad x_2/b_2 \rightarrow \kappa_2, \\ \frac{1}{4\pi\sqrt{e}\sqrt{\kappa_1+1}}n^{-1}b_1^{-1}b_2^{-1/2}x_2^{-1/2}f(\mathbf{x}) & \text{if } |x_1|/b_1 \rightarrow \kappa_1, \quad x_2/b_2 \rightarrow \infty, \end{cases}$$

for non-negative constants κ_1, κ_2 . Hence,

$$\begin{aligned} MISE\{\hat{f}_4(\mathbf{x})\} &= \frac{1}{4}b_1^2 \int \{x_1f^{11}(\mathbf{x})\}^2 d\mathbf{x} + \frac{1}{4}b_2^2 \int \{x_2f^{22}(\mathbf{x})\}^2 d\mathbf{x} \\ &\quad + \frac{1}{2}b_1b_2 \int |x_1|x_2f^{11}(\mathbf{x})f^{22}(\mathbf{x})d\mathbf{x} + o(b_1^2 + b_2^2) \\ &\quad + \frac{1}{4\pi\sqrt{e}}n^{-1}b_1^{-1/2}b_2^{-1/2} \int |x_1|^{-1/2}x_2^{-1/2}f(\mathbf{x})d\mathbf{x} \\ &\quad + o(n^{-1}b_1^{-1/2}b_2^{-1/2}). \end{aligned}$$

For $b_1 = b_2 = b_0$, the optimal b_0 is given by

$$\left[\frac{\frac{1}{4\pi\sqrt{e}} \int |x_1|^{-1/2}x_2^{-1/2}f(\mathbf{x})d\mathbf{x}}{\frac{1}{2} \int \{|x_1|f^{11}(\mathbf{x}) + x_2f^{22}(\mathbf{x})\}^2 d\mathbf{x}} \right]^{1/3} n^{-1/3}$$

and, therefore, the optimal AMISE is obtained as

$$\begin{aligned} AMISE_{opt} &= \frac{3}{2^{4/3}} \left[\int \left\{ |x_1|f^{11}(\mathbf{x}) + x_2f^{22}(\mathbf{x}) \right\}^2 d\mathbf{x} \right]^{1/3} \\ &\quad \left[\frac{1}{4\pi\sqrt{e}} \int |x_1|^{-1/2}x_2^{-1/2}f(\mathbf{x})d\mathbf{x} \right]^{2/3} n^{-2/3}. \end{aligned}$$

4 Simulation study

In simulation study, we consider $n = 100$ and 200 with 1,000 replications for the following target distributions of different shapes, where C, HN, N, Ga ,

Exp, LG, TN represent Cauchy, Half-Normal, Normal, Gamma, Exponential, Logistic and Truncated Normal (truncated at zero) distributions respectively. Here l, s, sh and rt respectively denote the location, scale, shape and rate of the corresponding distribution.

- 1) Product of $C(l = 0, s = 1)$ and $HN(s = 2)$, say, f_1 (Fig. 1).
- 2) Product of $0.2 \times N(l = -3, s = 1) + 0.6 \times C(l = 0, s = 1) + 0.2 \times N(l = 3, s = 1)$ and $Ga(sh = 3, s = 1)$, say f_2 (Fig. 2).
- 3) Product of $0.4 \times N(l = -3, s = 3) + 0.2 \times C(l = 0, s = 1) + 0.4 \times N(l = 3, s = 3)$ and $Exp(rt = 1)$, say f_3 (Fig. 3).
- 4) Product of $0.5 \times LG(l = -1, s = 0.5) + 0.5 \times LG(l = 1.5, s = 0.7)$ and $0.6 \times TN(l = 0, s = 0.5) + 0.4 \times TN(l = 1.3, s = 0.25)$, say f_4 (Fig. 4).

For comparison among different kernel density estimators, the bandwidths are considered within a range such that $h = b = \sqrt{(b_1)} = \sqrt{(b_2)} = h_1 = h_2$; where $(h_1, h_2)^T$ is the bandwidth vector corresponding to the product of two classical Gaussian $(0, 1)$ kernels, which produces the 5-th estimator denoted by \hat{f}_5 . In each replication the bandwidths are chosen by minimizing the integrated squared error; where the range of integration for each target distribution is specified such that the value of the bivariate density function is ignorable beyond the considered range. The arithmetic mean and the standard deviation of the integrated squared error (ISE) and the bandwidth vector (BW) are reported in Table 1.

From the table it is observed, as expected, that with increasing sample size, the mean of ISE and BW of all estimators are decreasing for all target distributions considered. As we can see, \hat{f}_4 performs best in all situations and \hat{f}_3 does worst among the first four estimators. \hat{f}_2 performs second best for the first three target distributions, whereas with distribution f_4 , \hat{f}_2 outperforms \hat{f}_1 for $n = 100$, but is dominated by \hat{f}_1 for $n = 200$. This is because \hat{f}_1 asymptotically performs better than \hat{f}_2 for distribution f_4 , and the required convergence rate is reached at $n = 200$. The first four estimators perform significantly better than \hat{f}_5 reflecting the boundary bias problem of classical kernels, except for distribution f_2 , where \hat{f}_1 and \hat{f}_3 have mean ISE very close to that of \hat{f}_5 . In fact, \hat{f}_3 is outperformed by \hat{f}_5 , because distribution f_2 has low density near boundary of the non-negative variable, and hence the boundary bias of \hat{f}_5 comes out to be close to the biases of \hat{f}_1 and \hat{f}_3 .

5 Application

Applicability of density estimator \hat{f}_4 is demonstrated using two sets of astronomical data. For given data set $\mathbf{X}_1 = (X_{11}, X_{12})^T, \dots, \mathbf{X}_n = (X_{n1}, X_{n2})^T$ of size n , the bandwidths are selected by minimizing

$$\int \hat{f}^2(\mathbf{x})d\mathbf{x} - \frac{2}{n^2} \sum_i \hat{f}_{-i}(\mathbf{X}_i),$$

where $\hat{f}_{-i}(\mathbf{X}_i)$ is an estimate of the target distribution f at the point \mathbf{X}_i , based on the given data set excluding the observation \mathbf{X}_i .

Our first data set consists of information on gamma-ray bursts (GRBs), the brightest explosion in the universe to date since the Big Bang (see, for example, Modak et al. 2018). We collect data from the fourth BATSE Gamma-Ray Burst Catalog (revised) (Paciesas et al., 1999) for the variable T_{90} , a measure of burst duration, is the time in second within which 90% of the flux arrive, and the variable P_{256} , peak flux measured in count per square centimeter per second on the 256 millisecond time scale, on 1496 long-duration GRBs (i.e. GRBs with $T_{90} > 2$ seconds). As usually done in astronomical studies to analyze the data set with huge variation in the values of the variables, we also consider the logarithm transformation of the variables, and study the relation between $\log_{10}(T_{90})$ and $\log_{10}(P_{256})$ (see, Fig. 5). Fig. 6 shows their bivariate density, estimated by \hat{f}_4 , corresponds to a multimodal distribution.

Next data set contains information on 1131 early-type galaxies (ETGs) at redshift (z) ranging from 0.06 to 2.67 (see, for example, Modak et al. 2017), where the data is collected from Förster et al., 2009; Saracco et al., 2009; Taylor et al., 2010; Damjanov et al., 2011; Papovich et al., 2012; Chen et al., 2013; McLure et al., 2013, and Szomoru et al., 2013. Fig. 7 shows the plot of $\log_{10}Re$ (Re : effective radius in kiloparsec) versus z for the galaxies, and the corresponding bivariate density estimated by \hat{f}_4 is shown in Fig. 8. The latter figure indicates two significantly different patterns in the density function, in which there is a high density function for the nearby ETGs, i.e. galaxies with redshift close to zero, and a low density function for the ETGs in higher redshift region.

6 Discussion

We consider the estimation of a bivariate density function with support $\mathfrak{R} \times [0, \infty)$ using the product of classical and associated kernels. We also suggest two new nonparametric density estimators based on *NG* kernels. The proposed estimators are proved to be free from boundary bias, whereas simulation study shows the estimator \hat{f}_4 performs best among its possible competitors. Practical implementation of estimator \hat{f}_4 includes two important fields of astronomical study, viz. GRB and ETG. In simulation, the bandwidth vector is selected by optimization method such that the integrated squared error is minimized. With increasing dimension, even if for the bivariate case, this selection procedure can be time consuming. Hence a fast algorithm is needed and bandwidth selection based on the specific kernel estimator is also desired. A search for full bandwidth matrix instead of diagonal matrix can be an open problem for future work (see, for example, Kokonendji and Somé 2018).

Table 1: Simulation study of the kernel density estimators

Estimator	ISE (mean) $\times 10^6$	ISE (sd) $\times 10^6$	1 st BW (mean)	1 st BW (sd)	2 nd BW (mean)	2 nd BW (sd)
n= 100, distribution f_1						
\hat{f}_1	2, 984	1, 360	0.481	0.072	0.358	0.095
\hat{f}_2	2, 644	1, 435	0.520	0.090	0.576	0.158
\hat{f}_3	3, 058	1, 414	0.302	0.072	0.208	0.060
\hat{f}_4	2, 384	1, 282	0.230	0.070	0.390	0.113
\hat{f}_5	4, 476	1, 620	0.516	0.073	0.485	0.110
n= 200, distribution f_1						
\hat{f}_1	2, 024	893	0.418	0.053	0.283	0.071
\hat{f}_2	1, 720	880	0.447	0.068	0.483	0.142
\hat{f}_3	2, 108	954	0.247	0.050	0.169	0.042
\hat{f}_4	1, 608	822	0.184	0.052	0.341	0.097
\hat{f}_5	3, 278	1, 056	0.457	0.060	0.392	0.084
n= 100, distribution f_2						
\hat{f}_1	1, 700	475	1.105	0.463	0.211	0.072
\hat{f}_2	1, 607	460	1.035	0.425	0.249	0.074
\hat{f}_3	1, 720	566	0.950	0.444	0.116	0.052
\hat{f}_4	1, 480	469	0.719	0.348	0.176	0.044
\hat{f}_5	1, 716	464	1.015	0.432	0.722	0.148
n= 200, distribution f_2						
\hat{f}_1	1, 216	341	0.729	0.272	0.185	0.049
\hat{f}_2	1, 137	334	0.683	0.227	0.224	0.050
\hat{f}_3	1, 272	361	0.613	0.343	0.099	0.039
\hat{f}_4	1, 071	306	0.439	0.232	0.160	0.034
\hat{f}_5	1, 242	343	0.694	0.242	0.663	0.104
n= 100, distribution f_3						
\hat{f}_1	2, 271	990	1.611	0.442	0.151	0.053
\hat{f}_2	1, 985	1, 108	1.964	0.549	0.204	0.056
\hat{f}_3	2, 303	1, 094	1.115	0.428	0.081	0.039
\hat{f}_4	1, 701	1, 037	1.035	0.396	0.126	0.048
\hat{f}_5	4, 160	1, 301	1.987	0.521	0.173	0.069
n= 200, distribution f_3						
\hat{f}_1	1, 667	669	1.293	0.374	0.128	0.040
\hat{f}_2	1, 439	722	1.580	0.487	0.177	0.050
\hat{f}_3	1, 663	731	0.881	0.343	0.067	0.030
\hat{f}_4	1, 207	653	0.846	0.319	0.107	0.037
\hat{f}_5	3, 207	909	1.754	0.445	0.137	0.057
n= 100, distribution f_4						
\hat{f}_1	10, 941	2, 417	0.729	0.191	0.071	0.039
\hat{f}_2	10, 791	2, 347	0.738	0.212	0.151	0.153
\hat{f}_3	11, 875	2, 791	0.429	0.173	0.045	0.025
\hat{f}_4	10, 574	2, 420	0.333	0.150	0.085	0.055
\hat{f}_5	12, 308	3, 115	0.749	0.179	0.147	0.039
n= 200, distribution f_4						
\hat{f}_1	8, 183	1, 863	0.593	0.120	0.048	0.024
\hat{f}_2	8, 339	1, 889	0.619	0.132	0.075	0.081
\hat{f}_3	8, 860	2, 185	0.295	0.101	0.034	0.015
\hat{f}_4	8, 101	1, 867	0.248	0.091	0.056	0.029
\hat{f}_5	9, 322	2, 262	0.607	0.113	0.124	0.024

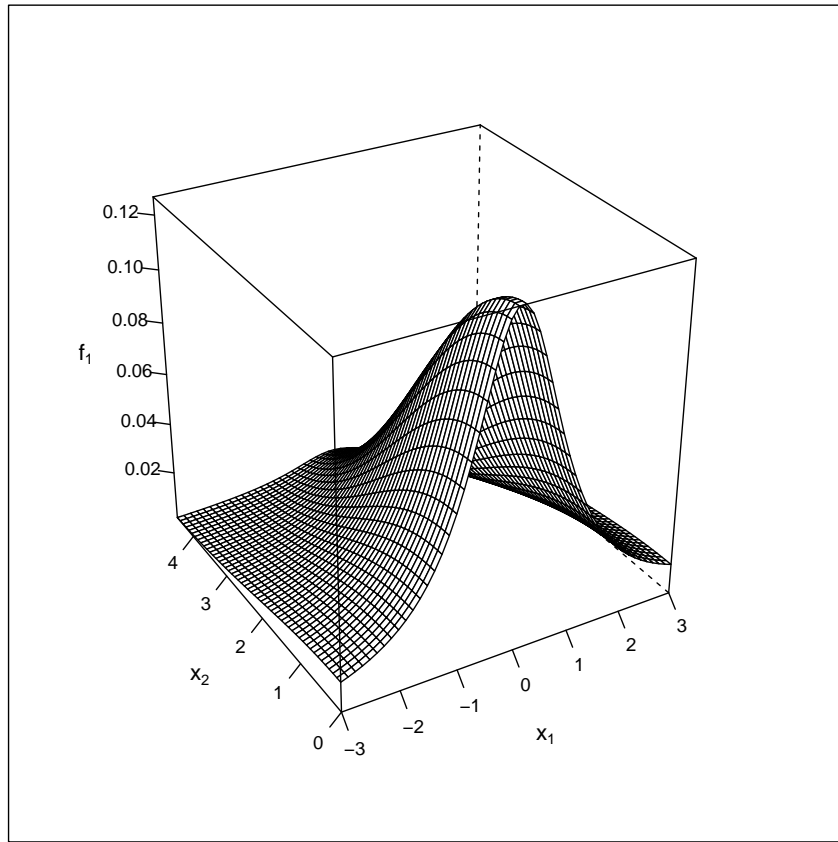


Figure 1: Surface plot of the distribution f_1 .

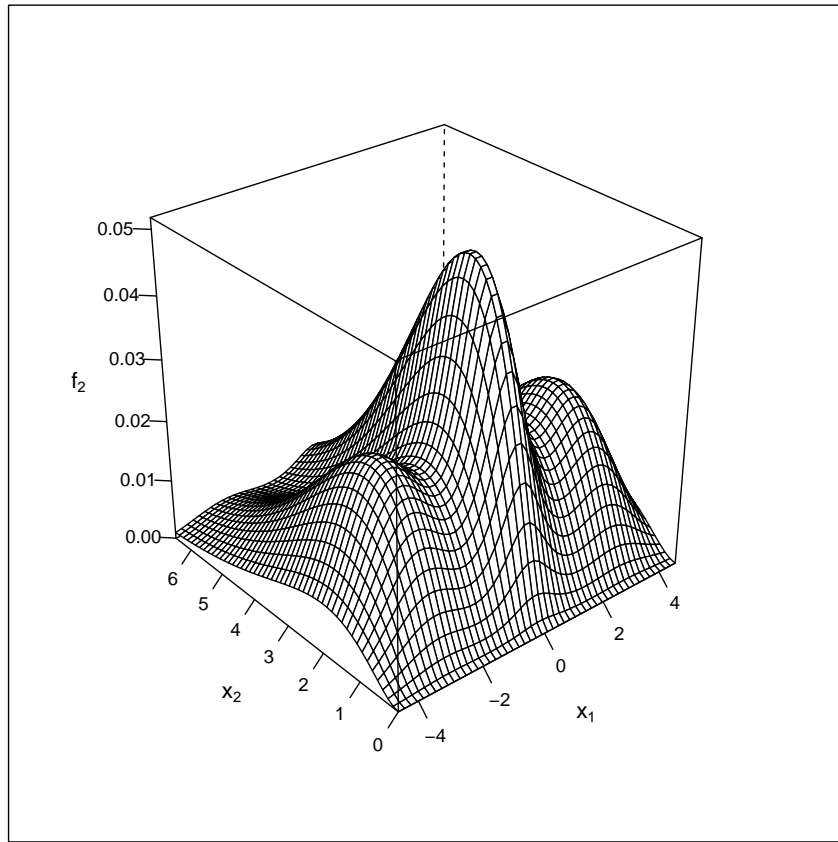


Figure 2: Surface plot of the distribution f_2 .

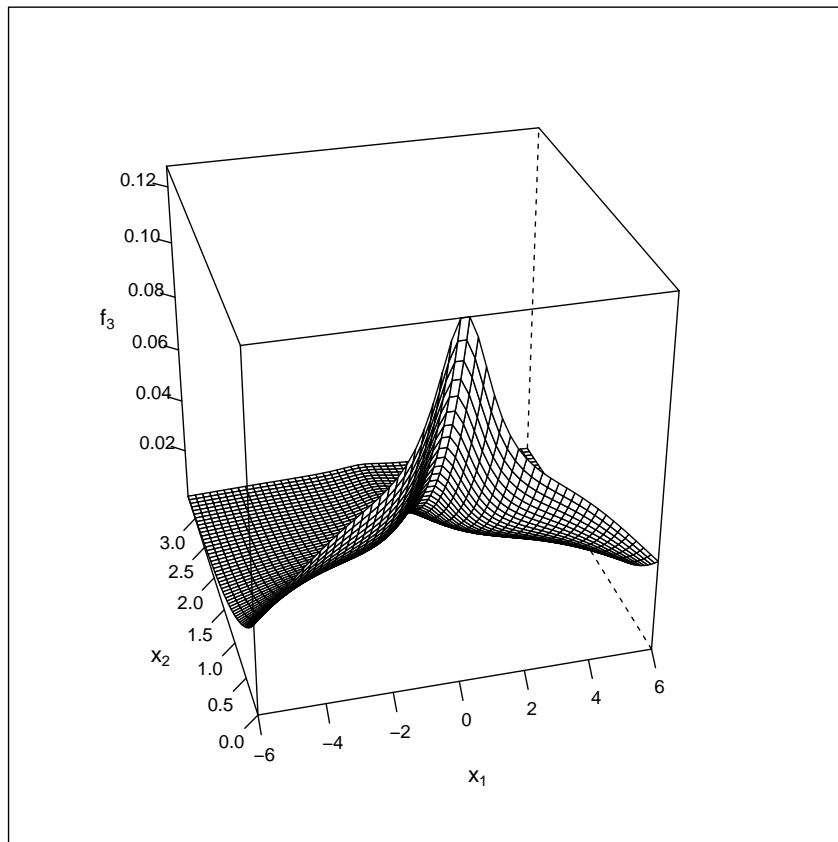


Figure 3: Surface plot of the distribution f_3 .

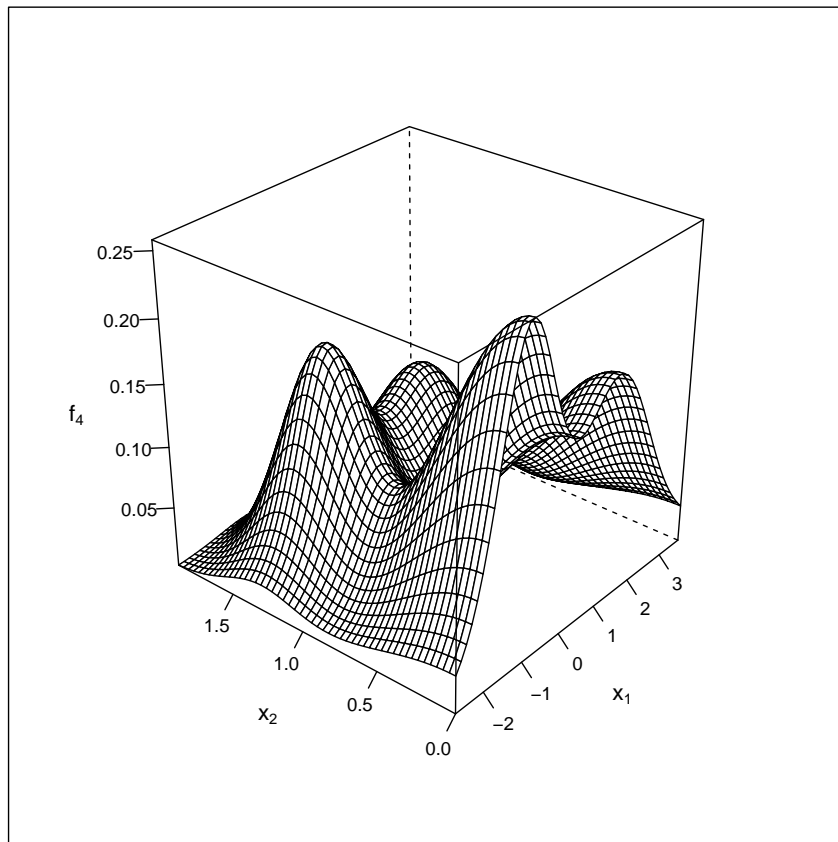


Figure 4: Surface plot of the distribution f_4 .

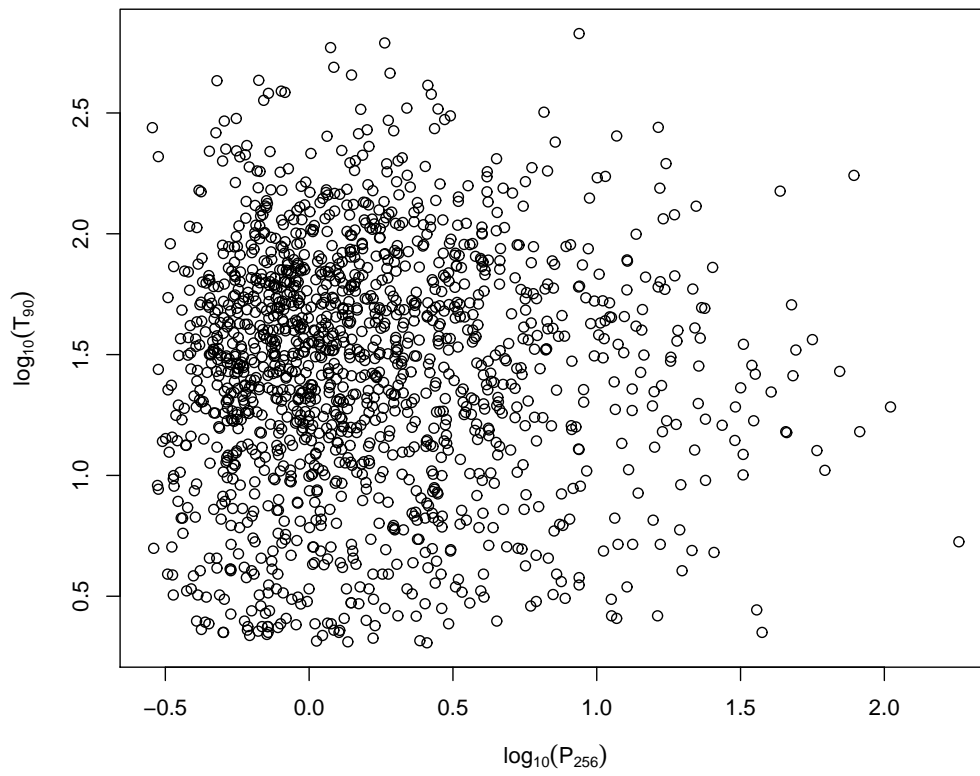


Figure 5: Scatter plot of the GRB data set.

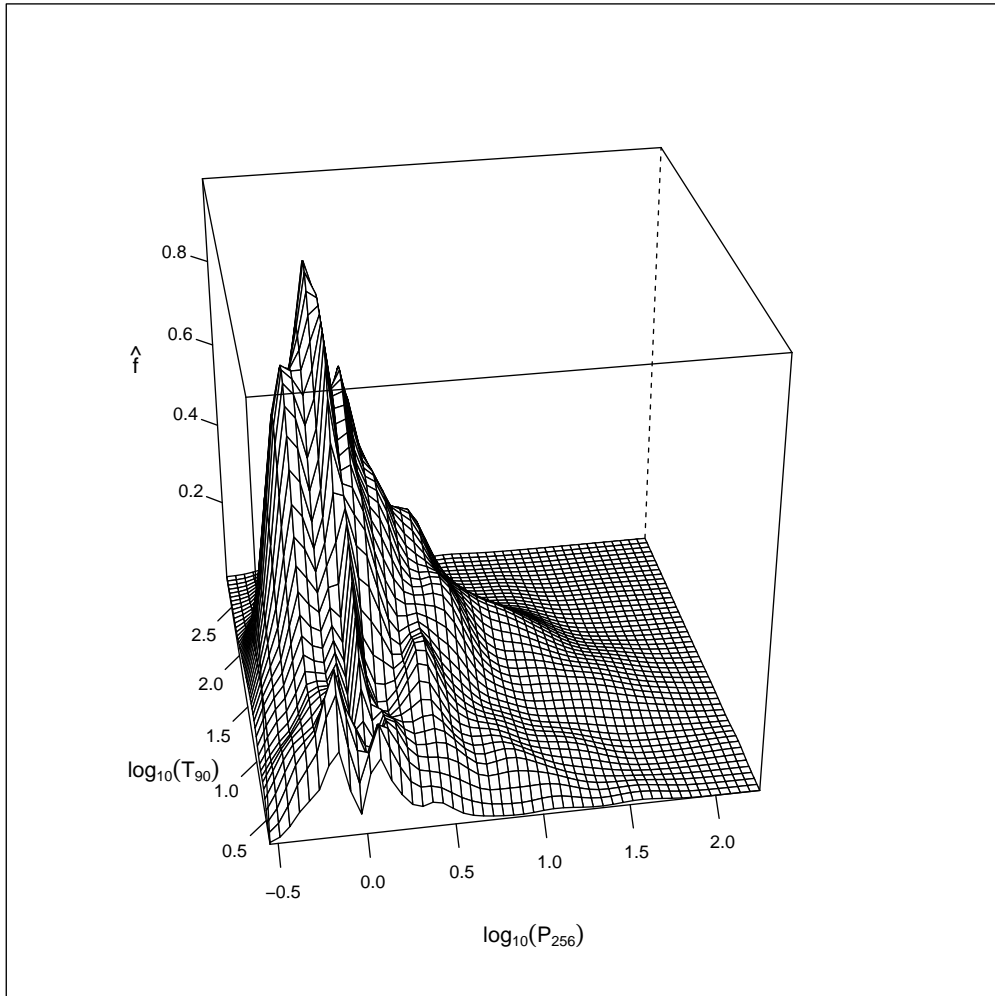


Figure 6: Surface plot of the density of GRB data set, estimated by \hat{f}_4 with $BW = (0.013, 0.016)$.

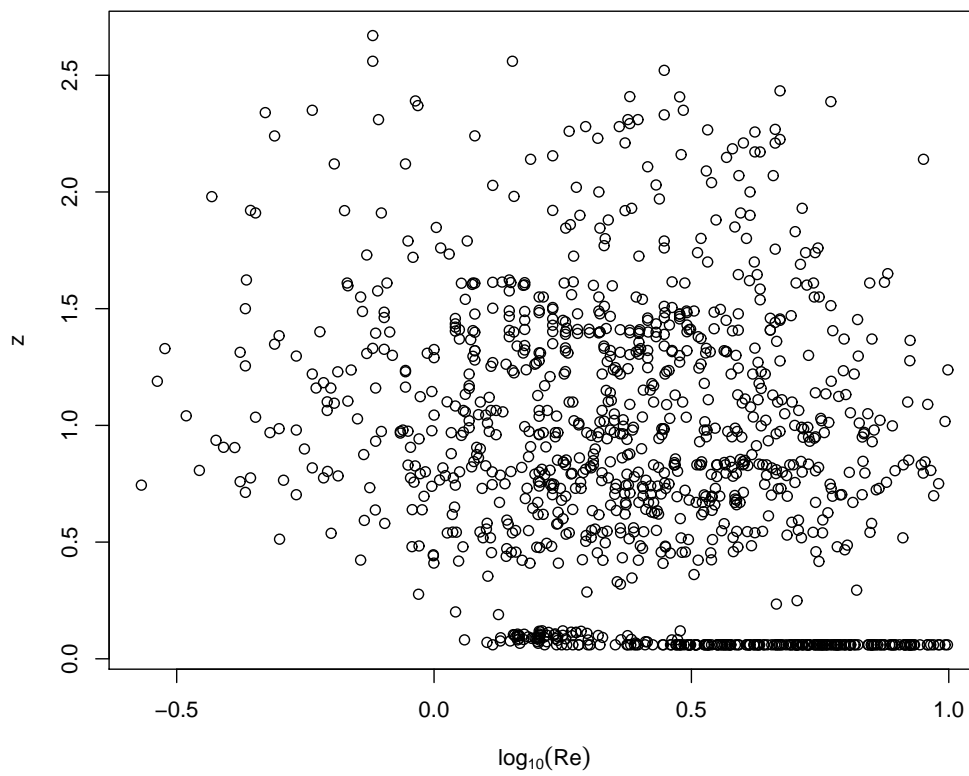


Figure 7: Scatter plot of the ETG data set.

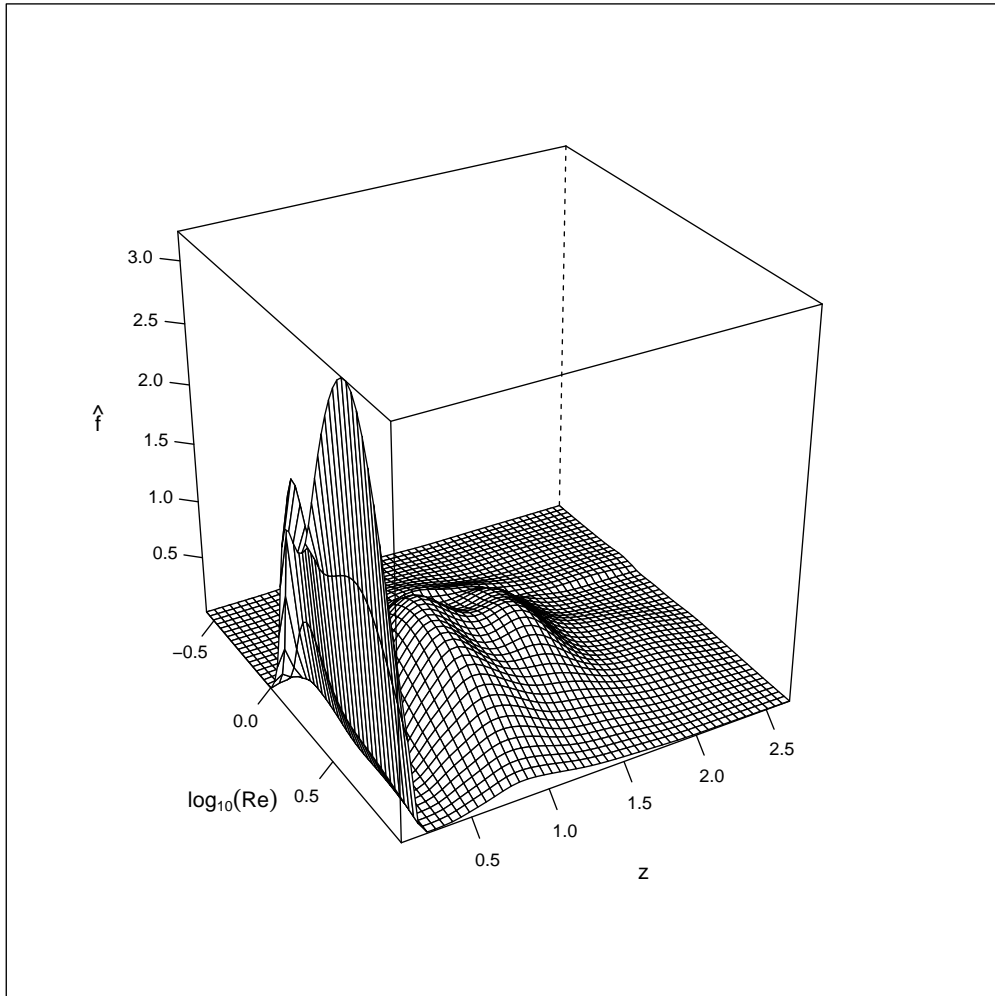


Figure 8: Surface plot of the density of ETG data set, estimated by \hat{f}_4 with $\text{BW} = (0.02, 0.02)$.

Appendix

A.1

$$\begin{aligned}
\{E_{\xi_{x_1}, \xi_{x_2}}(\xi_{x_1} - x_1)\}f^1(\mathbf{x}) &= f^1(\mathbf{x})\{E_{\xi_{x_1}|\xi_{x_2}, \xi_{x_2}}(\xi_{x_1} - x_1)\} \\
&= f^1(\mathbf{x}) \left[\int_{\xi_{x_1}} \int_{\xi_{x_2}} (\xi_{x_1} - x_1) N(\xi_{x_1}|\mu, (\lambda\xi_2)^{-1}) Ga(\xi_{x_2}|\alpha, \beta) d\xi_{x_1} d\xi_{x_2} \right] \\
&= f^1(\mathbf{x}) \left[\int_{\xi_{x_2}} \left\{ \int_{\xi_{x_1}} (\xi_{x_1} - x_1) N(\xi_{x_1}|\mu, (\lambda\xi_2)^{-1}) d\xi_{x_1} \right\} Ga(\xi_{x_2}|\alpha, \beta) d\xi_{x_2} \right] \\
&= f^1(\mathbf{x}) \left[\int_{\xi_{x_2}} \{E_{\xi_{x_1}|\xi_{x_2}}(\xi_{x_1} - E_{\xi_{x_1}|\xi_{x_2}}(\xi_{x_1}))\} Ga(\xi_{x_2}|\alpha, \beta) d\xi_{x_2} \right] \\
&= 0, \quad \text{since } \xi_{x_1}|\xi_{x_2} \text{ follows } N(\xi_{x_1}|\mu, (\lambda\xi_2)^{-1}).
\end{aligned}$$

Similarly,

$$\{E_{\xi_{x_1}, \xi_{x_2}}(\xi_{x_2} - x_2)\}f^2(\mathbf{x}) = 2b_2 f^2(\mathbf{x}).$$

Again,

$$\begin{aligned}
&\frac{1}{2}E\{(\xi_{x_1} - x_1)(\xi_{x_2} - x_2)\}f^{12}(\mathbf{x}) \\
&= \frac{1}{2}f^{12}(\mathbf{x}) \left[\int_{\xi_{x_2}} (\xi_{x_2} - x_2) \left\{ \int_{\xi_{x_1}} (\xi_{x_1} - x_1) N(\xi_{x_1}|\mu, (\lambda\xi_2)^{-1}) d\xi_{x_1} \right\} Ga(\xi_{x_2}|\alpha, \beta) d\xi_{x_2} \right] \\
&= 0.
\end{aligned}$$

Similarly,

$$\frac{1}{2}E\{(\xi_{x_1} - x_1)(\xi_{x_2} - x_2)\}f^{21}(\mathbf{x}) = 0.$$

Now,

$$\begin{aligned}
& \frac{1}{2}E\{(\xi_{x_1} - x_1)^2\}f^{11}(\mathbf{x}) \\
&= \frac{1}{2}f^{11}(\mathbf{x}) \left[\int_{\xi_{x_2}} \left\{ \int_{\xi_{x_1}} (\xi_{x_1} - x_1)^2 N(\xi_{x_1}|\mu, (\lambda\xi_2)^{-1}) d\xi_{x_1} \right\} Ga(\xi_{x_2}|\alpha, \beta) d\xi_{x_2} \right] \\
&= \frac{1}{2}f^{11}(\mathbf{x}) \left[\int_{\xi_{x_2}} \{Var_{\xi_{x_1}|\xi_{x_2}}(\xi_{x_1})\} Ga(\xi_{x_2}|\alpha, \beta) d\xi_{x_2} \right] \\
&= \frac{1}{2}f^{11}(\mathbf{x})\lambda^{-1} \left\{ \int_{\xi_{x_2}} \xi_{x_2}^{-1} Ga(\xi_{x_2}|\alpha, \beta) d\xi_{x_2} \right\}, \text{ as } Var_{\xi_{x_1}|\xi_{x_2}}(\xi_{x_1}) = (\lambda\xi_{x_2})^{-1} \\
&= \frac{1}{2}f^{11}(\mathbf{x})\lambda^{-1}(\alpha - 1)^{-1}\beta = \frac{1}{2}|x_1|f^{11}(\mathbf{x}).
\end{aligned}$$

Similarly,

$$\begin{aligned}
\frac{1}{2}E\{(\xi_{x_2} - x_2)^2\}f^{22}(\mathbf{x}) &= \frac{1}{2}f^{22}(\mathbf{x})\{Var(\xi_{x_2}) + (2b_2)^2\} \\
&= \frac{1}{2}f^{22}(\mathbf{x})(x_2b_2 + 6b_2^2), \text{ since } Var(\xi_{x_2}) = x_2b_2 + 2b_2^2.
\end{aligned}$$

A.2

$$\begin{aligned}
Var\{\hat{f}(\mathbf{x})\} &= n^{-1}Var\{K_{\Theta}(\mathbf{X}_i)\} \\
&= n^{-1}E\{K_{\Theta}(\mathbf{X}_i)\}^2 + O(n^{-1}).
\end{aligned}$$

Now,

$$\begin{aligned}
E_{\xi_{x_1}, \xi_{x_2}}\{K_{\Theta}(\mathbf{X}_i)\}^2 &= \int_{\xi_{x_2}} \left[\int_{\xi_{x_1}} \{N(\xi_{x_1}|\mu, (\lambda\xi_2)^{-1})\}^2 d\xi_{x_1} \right] \{Ga(\xi_{x_2}|\alpha, \beta)\}^2 d\xi_{x_2} \\
&= \frac{\sqrt{\lambda}\sqrt{\eta_{x_2}}}{2\sqrt{\pi}} N(\eta_{x_1}|\mu, (2\lambda\eta_{x_2})^{-1}) \{Ga(\xi_{x_2}|\alpha, \beta)\}^2 d\xi_{x_2} \\
&= B_{b_1, b_2}(x_1, x_2) N(\eta_{x_1}|\mu, (2\lambda\eta_{x_2})^{-1}) Ga(\eta_{x_2}|2\alpha - 1/2, 2\beta),
\end{aligned}$$

where $B_{b_1, b_2}(x_1, x_2) = \frac{\sqrt{\lambda} \sqrt{\Gamma(2\alpha-1/2)}}{\sqrt{\pi} 2^{2\alpha+1/2} \Gamma(\alpha)^2} \beta^{1/2}$. Then, writing the gamma function in terms of $R(z) = \sqrt{2\pi} e^{-z} z^{z+1/2} / \Gamma(z+1)$ for $z \geq 0$ we obtain,

$$\frac{\sqrt{\Gamma(2\alpha-1/2)}}{\Gamma(\alpha)^2} = \frac{1}{\sqrt{\pi e}} 2^{2\alpha-3/2} \left\{ 1 + \frac{1}{4(\alpha-1)} \right\}^{2\alpha-1} \frac{R^2(\alpha-1)}{R(2\alpha-3/2)},$$

which implies (Brown and Chen, 1999) $B_{b_1, b_2}(x_1, x_2) \leq \frac{1}{4\pi\sqrt{e}} \sqrt{\lambda\beta}$ for $\alpha \rightarrow \infty$. Therefore, $B_{b_1, b_2}(x_1, x_2)$ is approximated as

$$\begin{cases} \frac{1}{4\pi\sqrt{e}} b_1^{-1/2} b_2^{-1/2} |x_1|^{-1/2} x_2^{-1/2} & \text{if } x_1/b_1 \rightarrow \infty \text{ and } x_2/b_2 \rightarrow \infty, \\ \frac{\Gamma(2\kappa_2+7/2)}{\sqrt{\pi} 2^{2\kappa_2+9/2} \sqrt{(\kappa_1+1)(\kappa_2+1)\Gamma^2(\kappa_2+2)}} b_1^{-1} b_2^{-1} & \text{if } x_1/b_1 \rightarrow \kappa_1 \text{ and } x_2/b_2 \rightarrow \kappa_2, \\ \frac{\Gamma(2\kappa_2+7/2)}{\sqrt{\pi} 2^{2\kappa_2+9/2} \sqrt{(\kappa_2+1)\Gamma^2(\kappa_2+2)}} b_1^{-1/2} b_2^{-1} |x_1|^{-1/2} & \text{if } x_1/b_1 \rightarrow \infty \text{ and } x_2/b_2 \rightarrow \kappa_2, \\ \frac{1}{4\pi\sqrt{e}\sqrt{\kappa_1+1}} b_1^{-1} b_2^{-1/2} x_2^{-1/2} & \text{if } x_1/b_1 \rightarrow \kappa_1 \text{ and } x_2/b_2 \rightarrow \infty, \end{cases}$$

for non-negative constants κ_1, κ_2 .

A.3

Now, for $\delta_1 = b_1^{1-\epsilon_1}$ with $0 < \epsilon_1 < 1$ and $\delta_2 = b_2^{1-\epsilon_2}$ with $0 < \epsilon_2 < 1$,

$$\begin{aligned}
& \int_{-\infty}^{\infty} \int_0^{\infty} \text{Var}\{\hat{f}_3(\mathbf{x})\} dx_1 dx_2 = 2 \int_0^{\infty} \int_0^{\infty} \text{Var}\{\hat{f}_3(\mathbf{x})\} dx_1 dx_2 \\
& = 2 \left[\int_0^{\delta_1} \int_0^{\delta_2} \text{Var}\{\hat{f}_3(\mathbf{x})\} dx_1 dx_2 + \int_0^{\delta_1} \int_{\delta_2}^{\infty} \text{Var}\{\hat{f}_3(\mathbf{x})\} dx_1 dx_2 \right. \\
& \quad \left. + \int_{\delta_1}^{\infty} \int_0^{\delta_2} \text{Var}\{\hat{f}_3(\mathbf{x})\} dx_1 dx_2 + \int_{\delta_1}^{\infty} \int_{\delta_2}^{\infty} \text{Var}\{\hat{f}_3(\mathbf{x})\} dx_1 dx_2 \right] \\
& = 2 \left[\frac{1}{4\pi\sqrt{e}\sqrt{\kappa_1+1}} n^{-1} b_1^{-1} b_2^{-1/2} \int_0^{\delta_1} \int_{\delta_2}^{\infty} x_2^{-1/2} f(\mathbf{x}) dx_1 dx_2 \right. \\
& \quad + \frac{\Gamma(2\kappa_2+7/2)}{\sqrt{\pi} 2^{2\kappa_2+9/2} \sqrt{(\kappa_2+1)} \Gamma^2(\kappa_2+2)} n^{-1} b_1^{-1/2} b_2^{-1} \int_{\delta_1}^{\infty} \int_0^{\delta_2} |x_1|^{-1/2} f(\mathbf{x}) dx_1 dx_2 \\
& \quad \left. + \frac{1}{4\pi\sqrt{e}} n^{-1} b_1^{-1/2} b_2^{-1/2} \int_{\delta_1}^{\infty} \int_{\delta_2}^{\infty} |x_1|^{-1/2} x_2^{-1/2} f(\mathbf{x}) dx_1 dx_2 + O(n^{-1} b_1^{-\epsilon_1} b_2^{-\epsilon_2}) \right] \\
& = 2 \left[\frac{1}{4\pi\sqrt{e}} n^{-1} b_1^{-1/2} b_2^{-1/2} \int_0^{\infty} \int_0^{\infty} |x_1|^{-1/2} x_2^{-1/2} f(\mathbf{x}) dx_1 dx_2 + o(n^{-1} b_1^{-1/2} b_2^{-1/2}) \right] \\
& = \frac{1}{4\pi\sqrt{e}} n^{-1} b_1^{-1/2} b_2^{-1/2} \int_{-\infty}^{\infty} \int_0^{\infty} |x_1|^{-1/2} x_2^{-1/2} f(\mathbf{x}) dx_1 dx_2 + o(n^{-1} b_1^{-1/2} b_2^{-1/2})
\end{aligned}$$

with $\int_{-\infty}^{\infty} \int_0^{\infty} |x_1|^{-1/2} x_2^{-1/2} f(\mathbf{x}) dx_1 dx_2$ finite.

References

- [1] Bernardo, J. M. and Smith, A. F. M. (2000), *Bayesian Theory*, John Wiley & Sons, Ltd, Chichester.
- [2] Bouezmarni, T. and Rombouts, J. V. K. (2010), *Nonparametric density estimation for multivariate bounded data*, Journal of Statistical Planning and Inference, **140**, 139-152.

- [3] Brown, B. M. and Chen, S. X. (1999), *Beta-Bernstein smoothing for regression curves with compact support*, Scandinavian Journal of Statistics, **26**, 47–59.
- [4] Chen, S. X. (1999), *A beta kernel estimation for density functions*, Computational Statistics and Data Analysis, **31**, 131-145.
- [5] Chen, S. X. (2000), *Probability density function estimation using gamma kernels*, Annals of the Institute of Statistical Mathematics, **52**, 471-480.
- [6] Chen, Z., Shu, C. G., Burgarella, D., Buat, V., Huang, J. -S., Luo, Z. J. (2013), *Properties and morphologies of Lyman break galaxies at $z \sim 1$ in the Chandra Deep Field South, inferred from spectral energy distributions*, Monthly Notices of the Royal Astronomical Society, **431**, 2080–2105.
- [7] Damjanov, I., Abraham, R. G., Glazebrook, K., McCarthy, P. J., Caris, E., Carlberg, R. G., Chen, H. -W., Crampton, D., Green, A. W., Jørgensen, I., Juneau, S., Le Borgne, D., Marzke, R. O., Mentuch, E., Murowinski, R., Roth, K., Savaglio, S., Yan, H. (2011), *Red Nuggets at High Redshift: Structural Evolution of Quiescent Galaxies Over 10 Gyr of Cosmic History*, The Astrophysical Journal, **739**, L44–L49.
- [8] Förster Schreiber, N. M., Genzel, R., Bouché, N., Cresci, G., Davies, R., Buschkamp, P., Shapiro, K., Tacconi, L. J., Hicks, E. K. S., Genel, S., Shapley, A. E., Erb, D. K., Steidel, C. C., Lutz, D., Eisenhauer, F., Gillessen, S., Sternberg, A., Renzini, A., Cimatti, A., Daddi, E., Kurk, J., Lilly, S., Kong, X., Lehnert, M. D., Nesvadba, N., Verma, A., McCracken, H., Arimoto, N., Mignoli, M., Onodera, M. (2009), *The SINS Survey: SINFONI Integral Field Spectroscopy of $z \sim 2$ Star-forming Galaxies*, The Astrophysical Journal, **706**, 1364–1428.
- [9] Igarashi, G. and Kakizawa, Y. (2014), *Re-formulation of inverse Gaussian, reciprocal inverse Gaussian, and BirnbaumSaunders kernel estimators*, Statistics & Probability Letters, **84**, 235–246.
- [10] Kokonendji, C. C. and Somé, S. M. (2018), *On multivariate associated kernels to estimate general density functions*, Journal of the Korean Statistical Society, **47**, 112-126.

- [11] Libengué, F. G. (2013), *Méthode Non-Paramétrique par Noyaux Associés Mixtes et Applications*, Ph.D. Thesis Manuscript (in French) to Université de Franche-Comté, Besançon, France & Université de Ouagadougou, Burkina Faso, June 2013, LMB no. 14334, Besançon.
- [12] McLure, R. J., Pearce, H. J., Dunlop, J. S., Cirasuolo, M., Curtis-Lake, E., Bruce, V. A., Caputi, K. I., Almaini, O., Bonfield, D. G., Bradshaw, E. J., Buitrago, F., Chuter, R., Foucaud, S., Hartley, W. G., Jarvis, M. J. (2013), *The sizes, masses and specific star formation rates of massive galaxies at $1.3 < z < 1.5$: strong evidence in favour of evolution via minor mergers*, Monthly Notices of the Royal Astronomical Society, **428**, 1088–1106.
- [13] Modak, S., Chattopadhyay, T. and Chattopadhyay, A. K. (2017), *Two phase formation of massive elliptical galaxies: study through cross-correlation including spatial effect*, Astrophysics and Space Science, **362**, 206–215.
- [14] Modak, S., Chattopadhyay, A. K. and Chattopadhyay, T. (2018), *Clustering of gamma-ray bursts through kernel principal component analysis*, Communications in Statistics– Simulation and Computation, **47**, 1088–1102.
- [15] Paciasas, W. S., Meegan, C. A., Pendleton, G. N., Briggs, M. S., Kouveliotou, C., Koshut, T. M., Lestrade, J. P., McCollough, M. L., Brainerd, J. J., Hakkila, J., Henze, W., Preece, R. D., Connaughton, V., Kippen, R. M., Malozzi, R. S., Fishman, G. J., Richardson, G. A., Sahi, M. (1999), *The fourth batse gamma-ray burst catalog (revised)*, The Astrophysical Journal Supplement Series, **122**, 465–495.
- [16] Papovich C., Bassett, R., Lotz, J. M., van der Wel, A., Tran, K. -V., Finkelstein, S. L., Bell, E. F., Conselice, C. J., Dekel, A., Dunlop, J. S., Guo, Y., Faber, S. M., Farrah, D., Ferguson, H. C., Finkelstein, K. D., Häussler, B., Kocevski, D. D., Koekemoer, A. M., Koo, D. C., McGrath, E. J., McLure, R. J., McIntosh, D. H., Momcheva, I., Newman, J. A., Rudnick, G., Weiner, B., Willmer, C. N. A., Wuyts, S. (2012), *CANDELS Observations of the Structural Properties of Cluster Galaxies at $z = 1.62$* , The Astrophysical Journal, **750**, 93–106.

- [17] Saracco, P., Longhetti, M. and Andreon, S. (2009), *The population of early-type galaxies at $1 < z < 2$ - new clues on their formation and evolution*, Monthly Notices of the Royal Astronomical Society, **392**, 718–732.
- [18] Silverman, B. W. (1986), *Density Estimation for Statistics and Data Analysis*, Chapman and Hall, London.
- [19] Szomoru, D., Franx, M., van Dokkum, P. G., Trenti, M., Illingworth, G. D., Labbé, I., Oesch, P. (2013), *The Stellar Mass Structure of Massive Galaxies from $z = 0$ to $z = 2.5$: Surface Density Profiles and Half-mass Radii*, The Astrophysical Journal, **763**, 73–83.
- [20] Taylor, E. N., Franx M., Glazebrook, K., Brinchmann, J., Van Der Wel A. and Van Dokkum P. G. (2010), *On the Dearth of Compact, Massive, Red Sequence Galaxies in the Local Universe*, The Astrophysical Journal, **720**, 723–741.
- [21] Wand, M.P. and Jones, M.C., 1995. *Kernel Smoothing*, Chapman and Hall, New York.